

doi:10.15199/48.2024.12.07

Effect of clamp-type surge protection circuit configurations on EMC emissions from a flyback converter

Abstract. This paper presents the effect of passive clamp type surge suppression circuits of a switching transistor in a flyback converter on the conducted and radiated emission levels from the power supply system. The flyback configuration is used in low- and medium-power inverters in domestic and industrial equipment. The results of the study can provide practical guidance to a wide range of electronics engineers designing switching power supplies. The power supply system, with a power output of 7.5 W and an output voltage of 5 V, was practically manufactured and tested in accordance with the current standards for permissible disturbance emissions applicable in an industrial environment. The tests were carried out under the conditions of an accredited EMC measurement.

Streszczenie. W artykule przedstawiono wpływ pasywnych obwodów przeciwprzebiegowych tranzystora przełączającego w przetwornicy typu flyback na poziomy emisji przewodzonej i promieniowanej z układu zasilania. Konfiguracja flyback jest stosowana w przetwornicach małej i średniej mocy w urządzeniach domowych i przemysłowych. Wyniki badania mogą stanowić praktyczną wskazówkę dla szerokiego grona inżynierów elektroników projektujących zasilacze impulsowe. Układ zasilacza o mocy wyjściowej 7,5 W i napięciu wyjściowym 5 V został praktycznie wykonany i przetestowany zgodnie z obowiązującymi normami dopuszczalnej emisji zaburzeń obowiązującymi w środowisku przemysłowym. Testy zostały przeprowadzone w warunkach akredytowanego laboratorium pomiarowego EMC. (Wpływ konfiguracji obwodu typu clamp ochrony przeciwprzebiegowej na emisje EMC z przetwornicy typu flyback)

Keywords: flyback converter, clamp circuits, radiated emission, conducted emission.

Słowa kluczowe: przetwornica flyback, obwody clamp, emisja promieniowana, emisja przewodzona.

Introduction

Switch-mode power converters have been increasingly used as power supplies in consumer and industrial applications for years, displacing traditional linear regulated power supplies. Designers of these types of systems are paying increasing attention to increasing the efficiency of the system while reducing the size of the device. There is also an increase in the frequency of operation, which has a direct impact on the size reduction [1]. Nowadays, thanks to inverters with or without a planar core [2], the size and weight of such devices have been significantly reduced [3]. The cost of the device is also one of the most important factors. It is common practice for manufacturers to simplify the circuitry to the minimum necessary to reduce the cost of the device. This practice is a frequent cause of equipment failure and a failure to comply with current EMC directives. Measures to improve EMC performance are often neglected, which, combined with the ubiquity of this type of power supply, results in a significant resultant level of disturbance emissions to human infrastructure. This phenomenon is particularly critical in industrial settings with a large number of stand-alone power supply devices. Due to this situation, there has recently been a trend for the design of switch mode power supplies to also take into account the requirements of the EMC directives. In this study, the recommendations of EMC standards applicable in an industrialised environment were used to assess the levels of disturbance emissions [4]. It is common practice to include an EMC filter in power supply systems consisting of a choke compensated for the summation component and the addition of two capacitors to improve the attenuation of the differential component. However, for high levels of conducted emissions from the power supply system, this solution is not sufficient [5]. Ferrite rings applied to the power supply cables are also used to reduce conducted disturbances generated by the power supply system [6], which is also often not an effective solution. The situation is similar for radiated disturbance. If it is difficult to reduce both conducted and radiated emissions, the tedious and costly process of finding ways to reduce the level of disturbance emitted from the power supply begins. In addition, a PFC (Power Factor Correction) block is now

increasingly used in power supplies to reduce the level of reactive power [7,8]. Nowadays, PFC circuits are increasingly being applied in inverter circuits, due to their availability in an integrated version and their ease of use in the circuit. Due to the reduction in cost and size of equipment in low-power power supplies of a dozen or a few tens of watts, this solution is not commonly used. It should be mentioned that many industrial and consumer applications contain low-power power systems. At this point, it is important to consider how to reduce the emitted disturbance level reaching the input filter. The disturbance largely depends on the harmonic content created during the electronic key switching process in the inverter. In current low- and medium-power power supply systems, the switching element is usually a MOSFET transistor controlled from the driver circuit. Elements used to limit overvoltages during key switching are circuits that form a voltage limiter between the source and the drain (clamp circuits) [9]. In simple low-budget power supplies, these are circuits containing passive elements in a suitable configuration. In more complex power supplies, especially higher power supplies, appropriately controlled active elements are used in clamp circuits [10,11]. The configuration of such circuits determines the final shape of the source drain voltage (U_{DS}) and thus the content and distribution of the harmonic waveform [12]. Thus, there is a rationale that by selecting an appropriate circuit limiting the drain voltage U_{DS} , it is possible, in addition to reducing overvoltages, to reduce the level of conducted and radiated disturbances emitted by the power supply. Obviously, when designing an inverter circuit, the key requirement here is to reduce the voltage to an acceptable U_{DS} value using clamp type circuits. However, there is a wide variety of choices for this type of circuit and quite a significant margin in the designer's choice of U_{DS} voltage limit, enabling the selection of a clamp circuit with an optimum topology. This choice should be a compromise between transistor protection and EMC emission. Such a solution may result in a less critical selection of a less expensive line filter, taking up less valuable space in the device.

1. Implementation of the device

1.1 Selection of the inverter configuration.

Designers of small power converters (up to 100W) like to use power supply circuits in integrated form. The specialised circuit contains all the blocks of the converter, including the executive switch transistor, usually of the MOSFET type. Such a solution greatly simplifies the construction of the device, significantly reducing implementation costs. There are even dedicated programmes (calculators) for calculating the values and parameters of discrete elements cooperating with the circuit. This is also the solution adopted for the circuit in question. Here, the popular NCP1014 integrated circuit from ON Semiconductor [13] was used, adapted to realise switching power supplies in a two-bar flyback configuration [14,15,16]. The block diagram of such a solution is shown in fig.1. The mains voltage is rectified in a full-cycle Graetz rectifier and pre-filtered in capacitor C. In the first duty cycle, when the transistor (located in the driver block) is switched on, a current flows through the primary winding of the transformer. Then the magnetic flux in the core increases and energy is stored in the transformer. The voltage of the secondary winding polarises diode D in the rectifier in a negative way and energy is supplied to the load from capacitor C1 connected to the output. The output voltage rectifier with filter circuit gives a DC voltage at the output of the circuit. When the driver executive transistor is switched off then the magnetic flux in the core decreases. The secondary winding voltage polarises the output rectifier diode in the conduction direction and the secondary winding current flows through the load and recharges the output capacitance. The output voltage V_{out} is fed into a galvanically separated feedback circuit (e.g. an optotransistor) and controls the driver circuit to maintain the output voltage V_{out} at a preset level. When applying the transformer, it is important to bear in mind the relationship of the start and end windings, as indicated by dots in the figure. Optionally, an EMI filter is attached to the driver circuit to reduce the level of conducted disturbances emitted from the driver circuit to the permissible values specified in the standard [4].

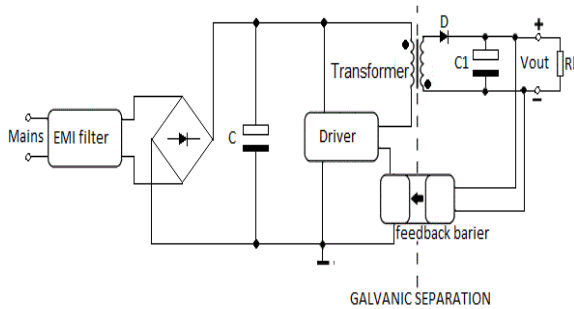


Fig.1. Block diagram of a flyback converter with galvanic separation at the output

Based on the information provided in the application note and general information on inverter design [13,17], a circuit was constructed and is shown in fig.2. The power supply operates in Discontinuous Conduction Mode (DCM). In this case, all the energy stored in the primary winding during the conduction of the keying transistor is given back to the load before the next cycle of the circuit starts [18,19]. The central part of the power supply is the NCP1014 integrated circuit. It contains in its structure the complete pulse power supply circuit including the driver and the MOSFET executive transistor. The maximum drain-source voltage of the transistor is 700V. The frequency of the internal oscillator is fixed at 100kHz. Due to the minimisation of power consumption in the stand-by mode of

the converter, it was decided to make an additional winding in the transformer design used to power the IC [13,14].

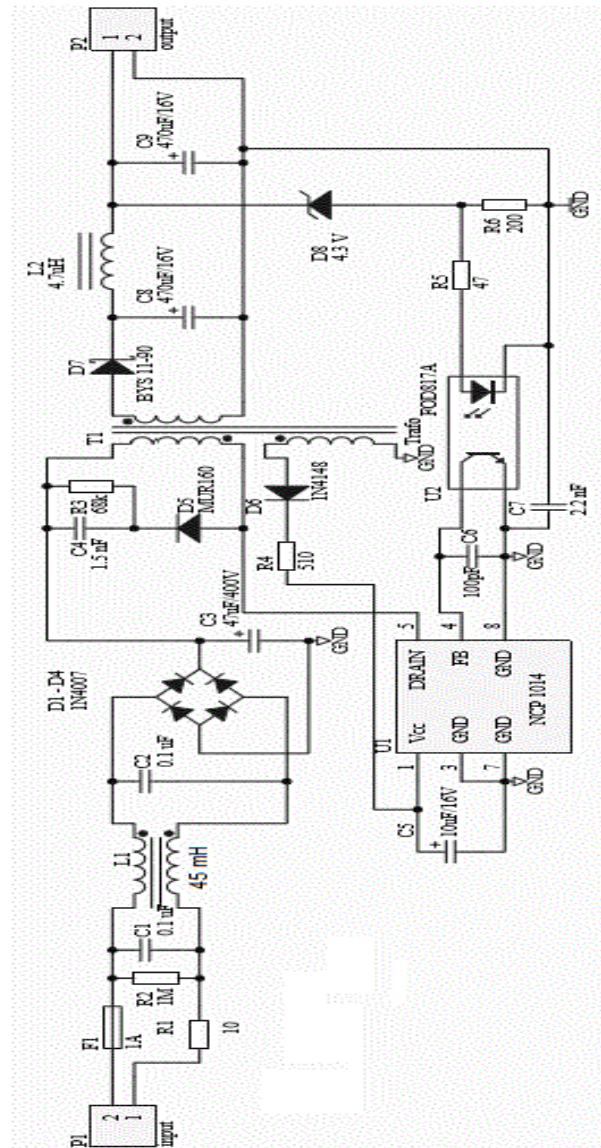


Fig.2. Schematic diagram of the realised inverter with a clamp type RCD surge protector

Due to its low price, it can be used in many low-budget solutions. Looking at the schematic diagram of the power supply, fig.2, at the input connected to the mains supply, there is a filter choke composed of C1, C2 elements and a compensated choke L1 [20]. The choke has a maximum impedance at 130kHz. The power supply is protected with a 1A fuse. Resistor R1 ensures that the current surge is reduced when the circuit is connected to the mains. Capacitor C3 reduces the DC voltage ripple obtained at the output of the Graetz bridge composed of diodes D1- D4. The circuit composed of diode D6, resistor R4 and electrolytic capacitor C5 constitutes the circuit providing the auxiliary voltage used to power the IC. The circuit presented in the diagram uses an RCD-type clamp circuit made up of resistor R3, capacitor C4 and fast rectifying diode D5. For the clamp circuit formed by the Zener diode and the fast diode, suitable solder pads on the printed circuit are used, connected, as is also the case for the RCD circuit, in parallel with the primary winding of the transformer. It is also possible to easily connect a capacitor in a clamp-type circuit consisting of capacitance alone. The circuit stabilises the output voltage in a negative feedback loop using

optotransistor U2, Zener diode D8, resistors R5 and R6 and capacitor C6. The DC output voltage is obtained in a rectifier composed of a Schottky diode and a π -type low-pass filter composed of capacitances C8 and C9 and choke L2. The printed circuit was designed according to common principles in the design of switching power supply boards [20,21,22].

The realised 7.5W inverter delivers an output voltage of 5V, with a maximum output current of 1.5 A and a ripple of 1.5 mV. The efficiency at a current consumption of $I_{out} = 1.5A$ is $\eta = 85\%$. A view of the finished converter is presented in fig.3.



Fig.3. View of the assembled converter

1.2 Clamp devices

If there is no clamp devices (snubber circuit), the MOSFET voltage stress during switching off the transistor will be very high. Its peak value could reach to [23]:

$$(1) V_s = I_p \sqrt{\frac{L_k}{C_p + C_{oss}}} + V_{in} + \frac{(V_{out} + V_f)}{N}$$

where: L_k – the leakage inductance; V_s – stress voltage; V_{in} – input voltage; V_{out} – output voltage; V_f – secondary diode forward voltage; C_p – primary winding capacitance in the transformer; C_{oss} – drain to source capacitance of the MOSFET; I_p – the maximum peak primary current; $N = N_p/N_s$ – turn ratio of transformer

This very high spike could cause bad EMI or even destroy the MOSFET. It would be worst at maximum I_p and V_{in} . When the transistor is switched off, the energy stored in inductance L_k causes voltage oscillations at the source-drain terminals, the frequency of which is determined by the relation [23]:

$$(2) f_{res} = \frac{1}{2\pi\sqrt{L_k(C_p + C_{oss})}}$$

Therefore, in practical applications, systems are required to reduce the overvoltages occurring in the transistor.

Three of the most popular passive clamp-type circuits [24] used in low-power inverters were used in this study. Their structure is shown in fig. 4. Circuit designers therefore have a choice between different circuit solutions, being able to select the one that will protect the circuit from electrical damage while ensuring low levels of electromagnetic disturbance emitted from the circuit. There are also applications for active clamp circuits, but they are used in higher power flyback circuits [25]. It is then possible to recover some of the loss power, which increases the efficiency of the power supply. The printed circuit design made it possible to freely change the configuration of the flyback circuits during measurements.

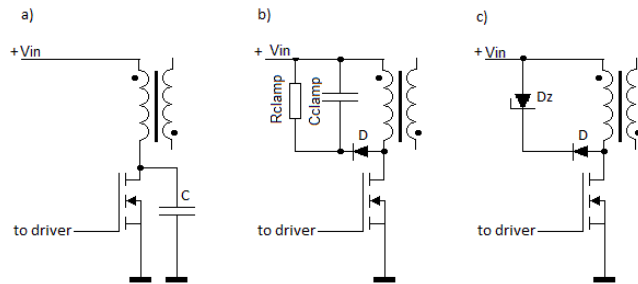


Fig.4. Clamp-type circuits to reduce voltage surges on a MOSFET-type switch transistor (a) with a capacitor attached to the drain (b) in an RCD-type circuit (c) with a Zener diode

• Single capacity system

The simplest of the circuits used (fig. 4a). The value of the capacitor C_{tot} connected to the drain end of the transistor can be determined from the relation [13]:

$$(3) V_d \max = V_{in} + N \cdot (V_{out} + V_f) + I_p \cdot \sqrt{\frac{L_k}{C_{tot}}}$$

where: C_{tot} – the total capacitance at the drain node

From an analysis of the relationship, it can be seen that an increase in capacitance results in a decrease in the maximum voltage occurring at the drain of the transistor. A capacitance of 220 pF was used in the model circuit.

The drain-source voltage waveform is shown in fig. 5, obtaining voltage values in accordance with the theoretical rationale in the literature [13].

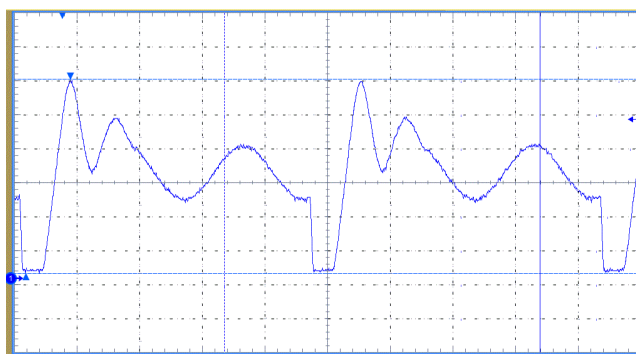


Fig.5. Drain source voltage waveform for capacitor; vertical 100V/div; horizontal 2µs/div. Maximum voltage value 560V.

• RCD device

When the switch is turned off, the transformer's leakage inductance sees two possible current paths: one through the output capacitance of the switch and one through the clamp circuit capacitor C_{clamp} . As the net capacitance that is seen is larger than it would be without the RCD snubber in the circuit, the voltage rise across the switch is slower and the eventual switch voltage is less. Energy that is transferred to C_{clamp} is transferred to R_{clamp} , which allows C_{clamp} to discharge so that its voltage does not become excessive.

The selection of R_{clamp} and C_{clamp} elements is made from dependencies expressed by the following formulas [13]:

$$(4) R_{clamp} = \frac{2 \cdot V_{clamp}(V_{clamp} - (V_{out} + V_f) \cdot N)}{L_k \cdot I_p^2 \cdot f_{sw}}$$

where: f_{sw} – switching frequency; V_{clamp} – usually selected 50-80V above the reflected value $N \cdot (V_{out} + V_f)$

$$(5) C_{clamp} = \frac{V_{clamp}}{V_{ripple} \cdot f_{sw} \cdot R_{clamp}}$$

In this system $R_{clamp} = 68 \text{ k}\Omega$, $C_{clamp} = 1.5 \text{ nF}$. A fast diode type MUR 160 was chosen as the diode. Fig. 6 shows the drain-source V_{DS} voltage waveform of a transistor, the shape of which is characteristic of a flyback converter operating in Discontinuous Conduction Mode and equipped with an RCD-type clamp circuit [26].

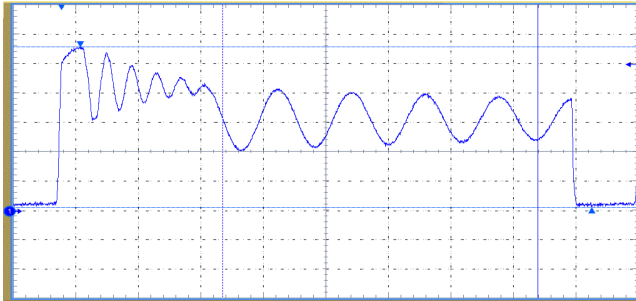


Fig.6. Drain source voltage waveform for RCD device; vertical 100V/div; horizontal 1µs/div. Maximum voltage value 540V.

• Zener or Transil diode

The circuit consists of a fast switching diode and a Zener diode or transil element (Transient Voltage Suppressor, TVS). The voltage of the Zener diode should be lower than the maximum drain-source voltage of the transistor less the maximum input voltage. However, the diode voltage should not be too low because it generates power losses in the diode. The maximum power loss in a Zener diode is represented by the relation [12]:

$$(6) P_{Zener} = \frac{1}{2} \cdot I_p^2 \cdot L_k \cdot \frac{V_{Zener}}{V_{Zener} - V_{out}} \cdot \frac{N_p}{N_s} \cdot f_{sw}$$

where: V_{Zener} – Zener voltage

The model solution uses a fast MUR 160 diode and a Zener diode type 1N5388B for a voltage of 200V and power 5W.

The drain to source voltage waveform of the system with a Zener diode is shown in fig. 7. The voltage waveform values obtained are in accordance with the predicted theoretical values [27].

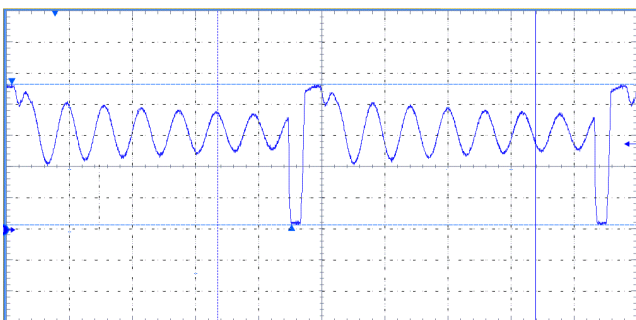


Fig.7. Drain source voltage waveform for Zener diode; vertical 100V/div; horizontal 2µs/div. Maximum voltage value 460V.

2. Measurements of disturbance emissions from a model inverter

Measurements were made in each case with an electromagnetic disturbance filter composed of C1, C2, L1 and R2 elements (fig. 2) connected at the mains input to the system. Measurements of radiated and conducted emissions were carried out for industrially acceptable levels,

according to the guidelines contained in standards [4]. Measurements were taken in an accredited EMC test laboratory. Tests were carried out with the system connected to a resistive load forcing the output current to flow at 1 A. This load value is representative of most practical applications. It is also a compromise in terms of the efficiency achieved and the level of electromagnetic disturbance emitted from the device. Several measurement series were performed for each of the three clamp circuits, with converging results. A view of the test bench for testing the conducted emission of the power supply is shown in fig. 8. Representative examples of the results obtained are shown below in subsections 2.1 and 2.2.

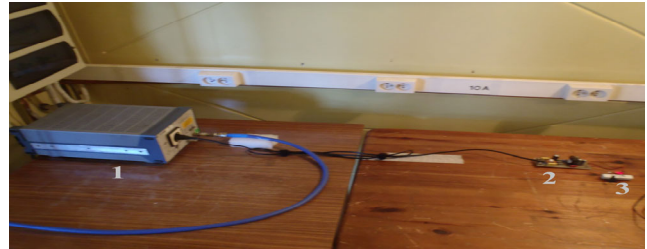


Fig.8. View of test stand for measurement of conducted disturbances from a switch mode power supply system 1 - artificial network, 2 - tested device, 3 – load

2.1 Radiated emission

Measurements were taken in a specialised shielding chamber located in an accredited testing laboratory. The distance between the measuring antenna and the test object in the form of a power supply was 3m each time. The system under test was devoid of a shielding enclosure, the presence of which would have affected the measurement. In addition to the disturbance signal itself, the electromagnetic background level in the chamber was also measured. This condition follows from standard [4]. The obtained results are presented in fig. 9, fig. 10 and fig. 11.

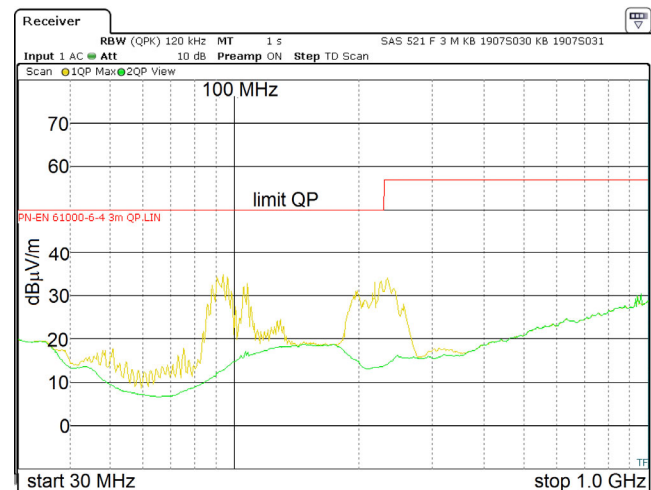


Fig.9. Radiated emission from a power supply system fitted with a clamp in RCD circuit; green -- background level; yellow - measurement result; red - limit

2.2 Conducted emission

The tests were performed in a shielding chamber. The converter system was connected to a single-phase artificial network cooperating with the measuring receiver. In this case, electromagnetic disturbances introduced into the mains are recorded. In each case, in accordance with the requirements of the standard, measurements were made with the detector Quasi-Peak and the Average. The relevant

detector limits are indicated in the figures. The obtained measurement results are presented in fig. 12, fig. 13 and fig.14.

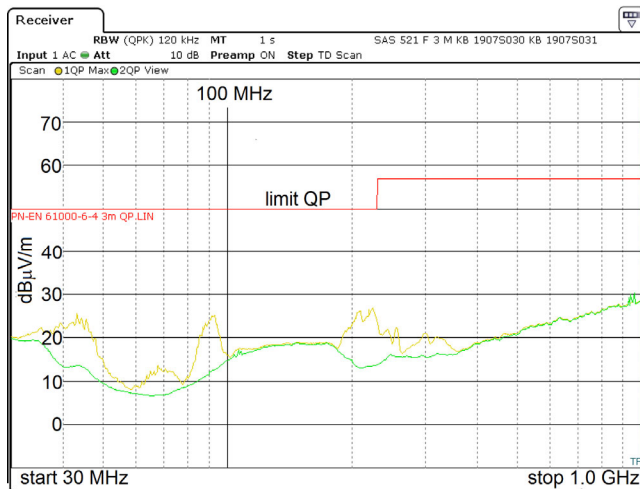


Fig.10. Radiated emission from a power supply system fitted with a capacitor clamp circuit; green -- background level; yellow - measurement result; red - limit

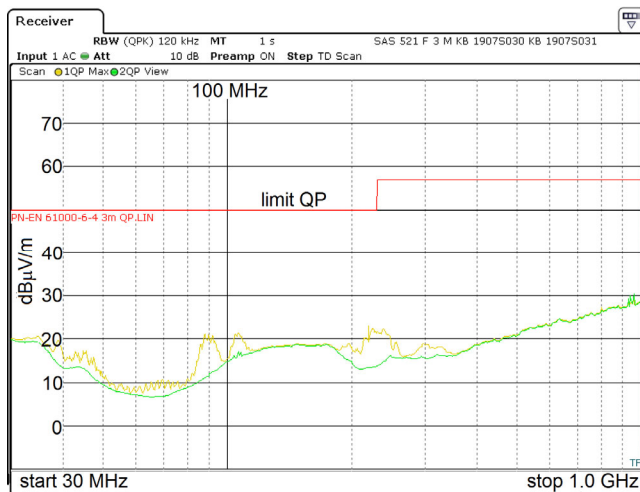


Fig.11. Radiated emission from a power supply circuit equipped with a clamp circuit with a Zener diode; green -- background level; yellow - measurement result; red - limit

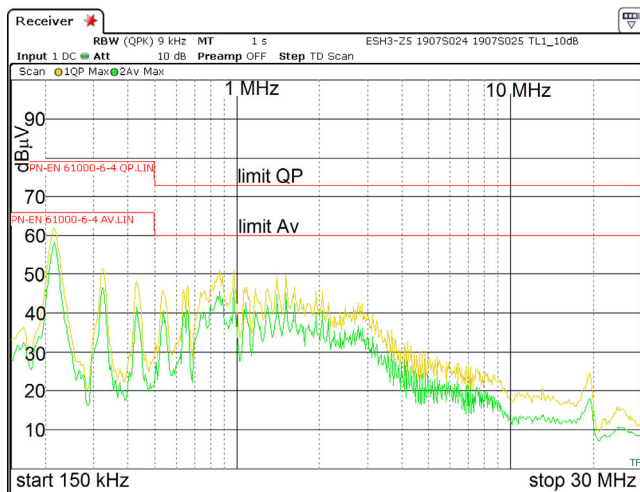


Fig.12. Conducted emission from a power supply system equipped with a clamp system with RCD circuit; yellow – QP measurement detector, green – Average measurement detector, red – limits

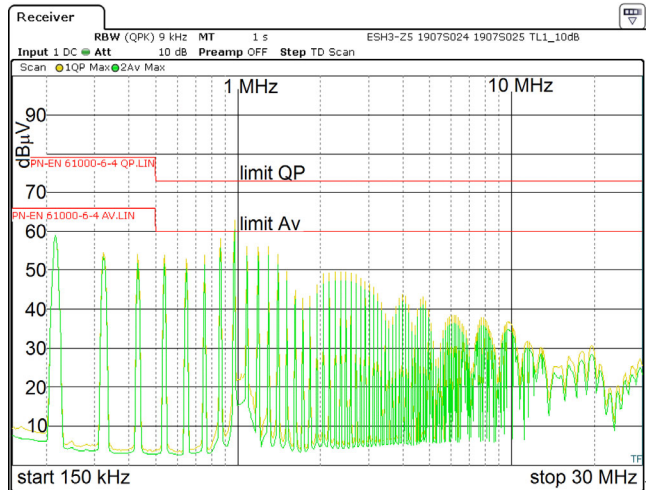


Fig.13. Conducted emission from a power supply system fitted with a capacitor clamp circuit; yellow – QP measurement detector, green – Average measurement detector, red – limits

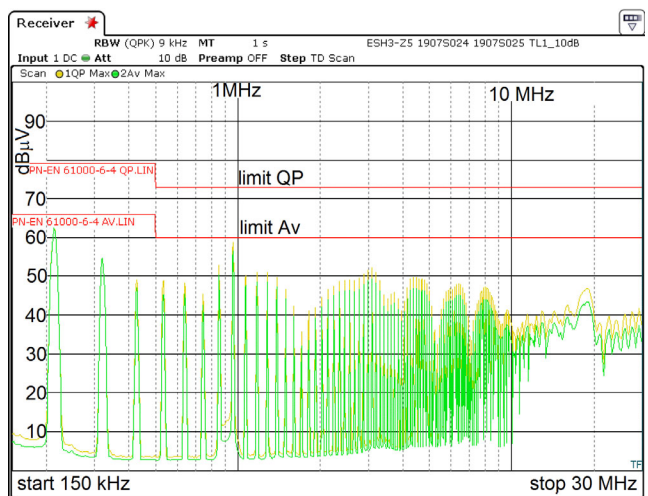


Fig.14. Conducted emission from a power supply circuit equipped with a clamp circuit with a Zener diode; yellow – QP measurement detector, green – Average measurement detector, red – limits

3. Conclusions

Three commonly used systems for reducing surges at the drain-source terminal of a MOSFET-type executive transistor operating in a flyback converter were considered. These were, respectively, an RCD circuit, a circuit with a Zener diode and a capacitor alone connected between the drain and source terminals of the MOSFET transistor. The evaluation of the level of emitted disturbances was made on the assumption that the inverter system operates under industrial conditions. According to PN 61000 - 6 - 4 [4], measurements of conducted disturbances in the range 0.15 - 30 MHz and radiated disturbances in the range 30 MHz - 1GHz are required. The measured object in the form of a converter in the above frequency ranges exhibits different disturbance propagation mechanisms. For conducted disturbances, there is the emission of disturbances directly into the power grid to which the power supply is galvanically connected. Radiated disturbance can affect the environment in the form of disturbance induction in cooperating equipment. In the radiated emissions study, the highest levels of disturbance were observed for the RCD-type clamp system. Smaller levels of disturbance were found for a system with a single capacitor and the smallest levels were measured for a system with a Zener diode. This situation is illustrated by the waveforms shown in figs. 9 - 11. The increased disturbance level for the clamp-type RCD

circuit can also be indirectly explained by the large size of the radiating elements taking up space on the board, which include a resistor, a capacitor and a diode. These elements form an array radiating electromagnetic waves in a kind of antenna. In other cases, it is a capacitor or two diodes. However, it should be noted that in none of the cases considered did the radiated emission exceed the permissible limits from the standard [4]. On each occasion, the interval exceeded the value of 15 dB, which can be considered a considerable margin. In the case of conducted emissions, which are measured in the lower frequency range, the lowest emission levels were obtained for the clamp system in the RCD configuration. Slightly higher, but still below the acceptable level, disturbances were found for the clamp circuit with Zener diode. For the clamp circuit with capacitive surge suppression, there is an overshoot of the permissible limit of 60 dB μ V in the vicinity of 1 MHz, as can be seen in fig. 13. In summary, a reasonable compromise between the levels of conducted and radiated disturbance is to choose a clamp type RCD. The use of such a solution guarantees lower maximum levels than required by the standard over a wide frequency range of 150 kHz - 1GHz. The second recommended clamp circuit is the Zener diode circuit, which ensures reduction of disturbances to acceptable levels in this frequency range. The downside of this solution is a particularly high level of conducted disturbance just below the permissible level. In the solution tested, the distance of the measured signal from the limit is small, and it is important to ensure, in accordance with good engineering practice, a minimum distance of 6 dB between the measured signal and the limit. It is not recommended to use a clamp circuit with only a capacitor switched between the drain and the transistor source. This solution does not provide a sufficient level of conducted disturbance reduction, which in the model device manifests itself by exceeding the permissible emission threshold in the vicinity of approximately 1 MHz. In addition, a clamp circuit with a Zener diode or capacitor emits significantly higher levels of conducted disturbance for frequencies greater than 1MHz at 40 - 50 dB μ V. For an RCD-type clamp circuit, this level for a frequency of 10 MHz is already only about 20 dB μ V. The economic factor of a more complex RCD system for small and medium volume production may not be decisive given the benefits of low disturbance levels, which translate into greater ease of compliance with EMC directives. This, in turn, saves valuable design time spent on the process of reducing disturbance from the device under construction. In high volume production, where the elimination of even one redundant component contributes to cost reduction, the use of a Zener diode circuit can also be considered.

Authors: dr inż. Krzysztof Maniak, National Institute of Telecommunications, Szachowa 1 street, 04-894 Warsaw E-mail: K.Maniak@il-pib.pl

REFERENCES

- [1] Hertel J.C., Nour Y., Knott A., Integrated very high frequency switch mode power supplies: design considerations, *IEEE Journal of Emerging and Selected Topics in Power Electronics*, vol. 6 (2017), No.2, 526 – 538, doi.org/10.1109/JESTPE.2017.2777884.
- [2] Tan L., Zhang M., Wang S., Pan S., Zhang Z., Li J., Huang X., The design and optimization of a wireless power transfer system allowing random access for multiple loads, *Energies*, vol.12 (2019), No.6, 1 – 19, doi.org/10.3390/en12061017
- [3] Knott A., Andersen T., P. Kamby P., Pedersen J.A., Madsen M.P., Kovacevic M., Andersen M.A.E., Evolution of very high frequency power supplies, *IEEE Journal of emerging and selected topics in power electronics*, vol. 2 (2013), No. 3, 386 – 394, doi:10.1109/JESTPE.2013.2294798
- [4] PN-EN IEC 61000-6-4:2019-12 Electromagnetic compatibility (EMC) - Part 6-4: General standards - Emission standard in industrial environments.
- [5] Hesener A., Electromagnetic Interference (EMI) in Power Supplies, Fairchild Semiconductor Power Seminar 2010-2011.
- [6] Suarez A., Victoria J., Torres J., Martinez P.A., Alcarria A., Perez J., Garcia-Olcina R., Soret J., Muetsch S., Gerfer A., Performance study of split ferrite cores designed for EMI suppression on cables, *Electronics*, vol. 9 (2020), No. 12, 1 – 19, doi.org/10.3390/electronics9121992
- [7] Cho K. S., Lee B. K., Kim J. S., CRM PFC Converter with New Valley Detection Method for Improving Power System Quality, *Electronics*, vol. 9 (2020), No. 1, 1 – 14, doi.org/10.3390/electronics9010038
- [8] Janesha J., Design of PFC converter with flyback converter and valley switching, in *Proc. 4th International Conference on Energy Efficient Technologies for Sustainability-ICEETS'18. St.Xavier's Catholic College of Engineering, Nagercoil, Tamil Nadu, India*, (2018), 1 – 12.
- [9] Milanovic M., Korelic J., Hren A., Mihalic F., Slibar P., Reduction of ringing losses in flyback converter by using the RC-RCD clamp circuit, *Automatika*, vol. 47 (2006), 31 – 37
- [10] Vracar D. D., Pejovic P. V., Active-clamp flyback converter as auxiliary power-supply of an 800V inductive-charging system for electric vehicles, *IEEE Access*, vol. 10 (2022), 38254 – 38271, doi:10.1109/ACCESS.2022.3165059
- [11] Bijeev N. V., Malhotra A., Jani V., Active clamp technique implementation for satellite electronic power conditioner, *International Journal of ICT Research & Development*, vol. 2 (2016), No. 7, 1 – 7
- [12] Ridley R., Flyback converter snubber design, *Switching Power Magazine*, (2005)
- [13] NCP1014 Self-supplied monolithic switcher for low standby-power offline SMPS, *ON Semiconductor application note* (2016)
- [14] Basso C., AND8125/D Evaluating the power capability of NCP101X members, *ON Semiconductor application note* (2003)
- [15] Gokcegoz F., Akboy E., Obdan A. H., Analysis and design of a flyback converter for universal input and wide load ranges, *Electrica*, vol. 21 (2020), No. 2, 235 – 241, doi:10.5152/electrica.2020.20092
- [16] Tanrikulu U., Akboy E., Akin B., Design and analysis of a flyback converter with improved snubber cells, *Sigma Journal of Engineering and Natural Sciences*, vol. 38 (2020), No. 4, 2205 - 2216
- [17] Pressman A. I., Billings K., Morey T., Switching power supply design, *The McGraw – Hill Companies*, (2009)
- [18] Kumar R., Wu C. C., Liu C. Y., Hsiao Y. L., W. H. Chieng W. H., Yi Chang E. Y., Discontinuous current mode modeling and zero current switching of flyback converter, *Energies*, vol. 14 (2021), No. 18, 1 – 23, doi.org/10.3390/en14185996
- [19] Singh B., Chaturvedi G. D., Analysis, Design and development of a single switch flyback buck-boost AC-DC converter for low power battery charging applications, *Journal of Power Electronics*, vol. 7 (2007), No. 4, 318 – 327
- [20] Maniktala S., "Switching Power Supplies A to Z," *Elsevier* (2006)
- [21] Maniak K., Tomczyk T, Electromagnetic compatibility in distributed power systems, *Przegląd Elektrotechniczny*, No. 2 (2018), 29 - 33, doi:10.15199/48.2018.02.08
- [22] Roberts S., DC/DC book of knowledge – practical tips for the user, *RECOM Engineering GmbH*, (2016)
- [23] Gao K., Goerke B. G., Chosing standard recovery diode or ultra-fast diode in snubber, *Application report SNVA744*, (2015)
- [24] Billings K., Switchmode power supply handbook, *The McGraw – Hill Companies*, (2009)
- [25] Pesce C., Riedemann J., Pena R., Jara W., Maury C., Villalobos R, A modified step-up DC-DC flyback converter with active snubber for improved efficiency, *Energies*, vol. 12 (2019), No. 11, 1 – 17, doi.org/10.3390/en12112066
- [26] Design guidelines for RCD snubber of flyback converters, *AN4147 Fairchild application note*.
- [27] Flyback Design Methodology, *Application Note AN-32. Power Integrations*, (2004)